

Electronic Supplementary Information

Enhancing oxygen reduction reaction activity of Pt-shelled catalysts via subsurface alloying

Daojian Cheng*, Xiangguo Qiu, and Haiyan Yu

State Key Laboratory of Organic-Inorganic Composites, Beijing University of Chemical
Technology, Beijing 100029, China

*Corresponding Author. E-mail address: chengdj@mail.buct.edu.cn (D. Cheng).

1. Computational methods

For the slab model, density-functional theory (DFT) calculations were performed by using the Vienna Ab-initio Simulation Package (VASP).¹⁻⁴ The spin-polarized generalized gradient approximation (GGA) with the Perdew-Wang (PW91) was used to describe the exchange and correlation potential.⁵ The cutoff energy for the plane-wave basis set was set to 400 eV in all calculations. The Monkhorst-Pack mesh k-points ($11 \times 11 \times 11$) and ($9 \times 9 \times 1$) were used for the bulk and slab calculations, respectively. The convergence criteria for the electronic self-consistent iteration and the ionic relaxation loop were set to 10^{-4} eV and 10^{-2} eV/Å, respectively. In DFT calculations, the slab alloys were modeled with a five-layer slab using a 2×2 supercell. A vacuum gap of about 20 Å in the z-direction was introduced to separate two subsequent slabs. The atoms in the top three layers were allowed to relax, while the atoms on the remaining two layers were fixed at their ideal bulk positions. All adsorbates were placed on one side of the slab.

For cluster model, all the DFT calculations were performed by using the Plane-Wave Self-Consistent Field (PWscf) plane wave DFT code in the quantum chemistry package Quantum Espresso 4.1.2.⁶ Spin-polarized calculations were performed using values of 40 and 320 Ry as the energy cut-off for the description of the wave function and the electronic density, respectively. The cluster was located in a $30 \times 30 \times 30$ Å cubic supercell. Only the gamma point in the Brillouin-zone (BZ) was used for the BZ integration of the clusters, while a Monkhorst-Pack grid⁷ of $8 \times 8 \times 8$ was used for the BZ integration of the bulk metals. The exchange and correlation interaction among electrons was described at the level of the generalized gradient approximation (GGA), using the Perdew-Burke-Ernzerhof (PBE) formula.⁸ Gaussian smearing method⁹ was employed to determine electron occupancies with a smearing parameter of 0.002 Ry. The positions of the atoms in the complex were fully optimized until the forces were smaller than 0.01 eV/Å per atom. The calculated fcc lattice constant of Pt (4.00 Å) is in good agreement with the measured value of 3.92 Å.¹⁰ The calculated bond length of a gas-phase oxygen molecule (1.24 Å) also agrees well with the experimental value 1.21 Å.¹⁰

2. The adsorption energies of atomic oxygen in the slab and cluster models.

The adsorption energy of atomic oxygen on the pure Pt(111) surface were calculated. The results were listed in Table S1. It is found that the fcc site is the most favorable one for atomic oxygen on the pure Pt(111) with an adsorption energy of about -4.69 eV, which is in good agreement with previous experimental and theoretical investigations.^{11, 12}

For the Pt-subsurface and Pt-skin alloy surfaces in the slab model, fcc, hcp, bridge, and top sites are considered, and the corresponding adsorption energies are listed in Tables S2 and S3, respectively. For the Pt₃M (M = Sc, Ti, V, Cr, Mn, Fe, Co, and Ni) alloy surfaces, six different adsorption sites: fcc-Pt₂M, fcc-Pt₃, hcp-Pt₂M, hcp-Pt₃, top-Pt, and top-M can be found, as shown in Fig. S1. Table S4 gives the corresponding adsorption energies of the Pt₃M alloy at different sites.

For the cluster model, three adsorption sites: top, bridge, and hollow are studied. Table S5 gives the corresponding adsorption energies of the Pt₁₂M and pure Pt₁₃ clusters at different sites.

3. Calculated d-band center of top-layer atoms of the different surface alloys

As d-band center position can approximately measure chemical activity of metallic catalysts, the d-band center of top-layer atoms of different slab alloys are calculated and are presented in Fig. S2. In general, there is a nearly linear trend in the adsorption energies versus the surface d-band center for the same alloy system with different alloy models. Definitely, for the same alloy system with different alloy models, the more negative d-band center, the weaker adsorption strength of oxygen atom.

REFERENCES

- 1 G. Kresse and J. Hafner, *Phys. Rev. B*, 1993, **47**, 558.
- 2 G. Kresse and J. Hafner, *Phys. Rev. B*, 1994, **49**, 14251.
- 3 G. Kresse and J. Furthmüller, *Comput. Mat. Sci.*, 1996, **6**, 15.
- 4 G. Kresse and J. Furthmüller, *Phys. Rev. B*, 1996, **54**, 11169.
- 5 J. P. Perdew, J. A. Chevary, S. H. Vosko, K. A. Jackson, M. R. Pederson, D. J. Singh and C. Fiolhais, *Phys. Rev. B*, 1992, **46**, 6671.
- 6 P. Giannozzi, S. Baroni, N. Bonini, M. Calandra, R. Car, C. Cavazzoni, D. Ceresoli, G. L. Chiarotti, M. Cococcioni and I. Dabo, *J. Phys. Condens. Matt.*, 2009, **21**, 395502.
- 7 H. J. Monkhorst and J. D. Pack, *Phys. Rev. B*, 1976, **13**, 5188.
- 8 J. P. Perdew, K. Burke and M. Ernzerhof, *Phys. Rev. Lett.*, 1996, **77**, 3865-3868.
- 9 M. Methfessel and A. T. Paxton, *Phys. Rev. B*, 1989, **40**, 3616-3621.
- 10 V. Branger, V. Pelosin, K. F. Badawi and P. Goudeau, *Thin Solid Films*, 1996, **275**, 22-24.
- 11 B. Han and G. Ceder, *Phys. Rev. B*, 2006, **74**, 205418.
- 12 U. Starke, N. Materer, A. Barbieri, R. Döll, K. Heinz, M. A. Van Hove and G. A. Somorjai, *Surf. Sci.*, 1993, **287-288**, 432-437.

Table S1 Adsorption energy (E_{ads} , in eV) of atomic oxygen on the pure Pt(111) surface and bond lengths of O-Pt ($d(\text{O-Pt})$, in Å) at different sites.

site	$d(\text{O-Pt})$		E_{ads}	
	this work	previous work ¹¹	this work	previous work ¹¹
top	1.83	1.84	-3.31	-3.08
hcp	2.05	2.06	-4.27	-4.19
fcc	2.05	2.05	-4.69	-4.67
Bridge	-	-	-	-

Table S2 Adsorption energies (E_{ads} , in eV) of atomic oxygen on the Pt-subsurface alloy surfaces at different sites.

	PtSc	PtTi	PtV	PtCr	PtMn	PtFe	PtCo	PtNi
bridge	-3.533	-3.453	-4.543	-4.677	-3.490	-2.922	-4.017	-
fcc	-3.329	-3.499	-4.498	-4.307	-2.847	-3.392	-4.002	-4.063
hcp	-3.535	-3.566	-4.496	-4.654	-3.092	-3.152	-3.759	-3.834
top	-2.555	-2.863	-3.838	-4.026	-2.613	-2.547	-3.005	-2.826

Table S3 Adsorption energies (E_{ads} , in eV) of atomic oxygen on the Pt-skin alloy surfaces at different sites.

	PtSc	PtTi	PtV	PtCr	PtMn	PtFe	PtCo	PtNi
bridge	-4.465	-4.340	-4.175	-4.325	-4.387	-4.271	-3.779	-
fcc	-4.471	-4.340	-4.175	-4.326	-4.385	-4.271	-4.311	-4.362
hcp	-4.078	3.861	-3.777	-3.960	-3.914	-3.874	-3.920	-4.102
top	-3.080	-2.927	-2.829	-2.954	-3.107	-2.991	-3.064	-3.952

Table S4 Adsorption energies (E_{ads} , in eV) of atomic oxygen on the Pt_3M alloy surfaces at different sites.

	PtSc	PtTi	PtV	PtCr	PtMn	PtFe	PtCo	PtNi
fcc-Pt₂M	-5.679	-5.873	-6.491	-5.626	-5.143	-4.990	-4.972	-4.719
fcc-Pt₃	-3.962	-3.384	-3.616	-4.010	-4.150	-4.266	-4.312	-4.501
hcp-Pt₂M	-5.427	-5.720	-6.492	-5.626	-4.404	-4.721	-4.715	-4.401
hcp-Pt₃	-4.484	-3.764	-3.790	-4.208	-4.394	-4.176	-4.203	-4.356
top-M	-3.935	-5.715	-6.491	-5.627	-4.435	-4.401	-4.130	-3.119
top-Pt	-4.482	-5.873	-6.490	-4.206	-4.389	-4.173	-4.206	-

Table S5 Adsorption energies (E_{ads} , in eV) of atomic oxygen on the Pt_{12}M and pure Pt_{13} clusters at different sites.

	Pt₁₂Sc	Pt₁₂Ti	Pt₁₂V	Pt₁₂Cr	Pt₁₂Mn	Pt₁₂Fe	Pt₁₂Co	Pt₁₂Ni	Pt₁₃
bridge	-0.299	-0.302	-0.314	-0.312	-0.290	-0.293	-0.278	-0.304	-0.324
hollow	-0.312	-0.325	-0.327	-0.332	-0.301	-0.307	-0.323	-0.313	-0.335
top	-0.260	-0.326	-0.349	-0.370	-0.258	-0.270	-0.278	-0.275	-0.337

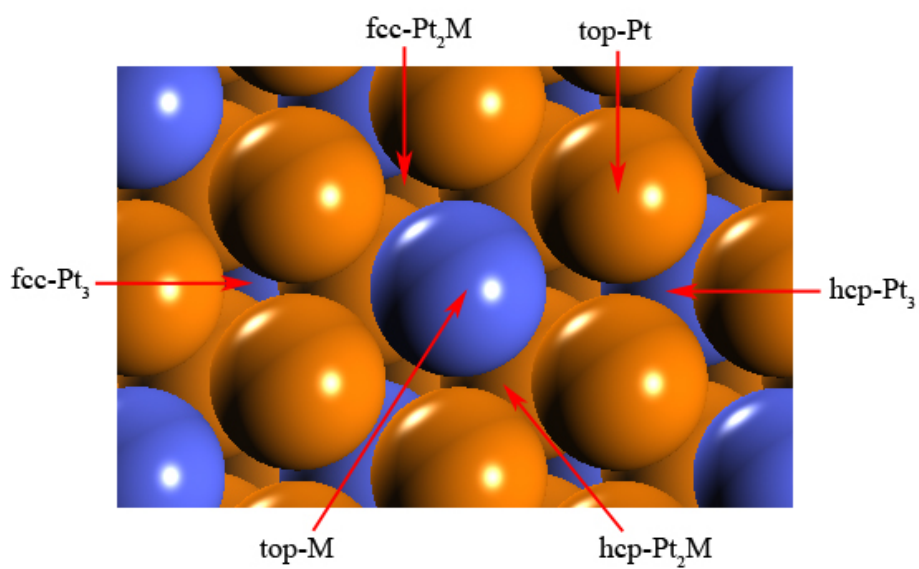


Fig. S1 Top view of the adsorption sites on Pt₃M alloy surface. Orange and blue spheres represent the Pt and M atoms, respectively.

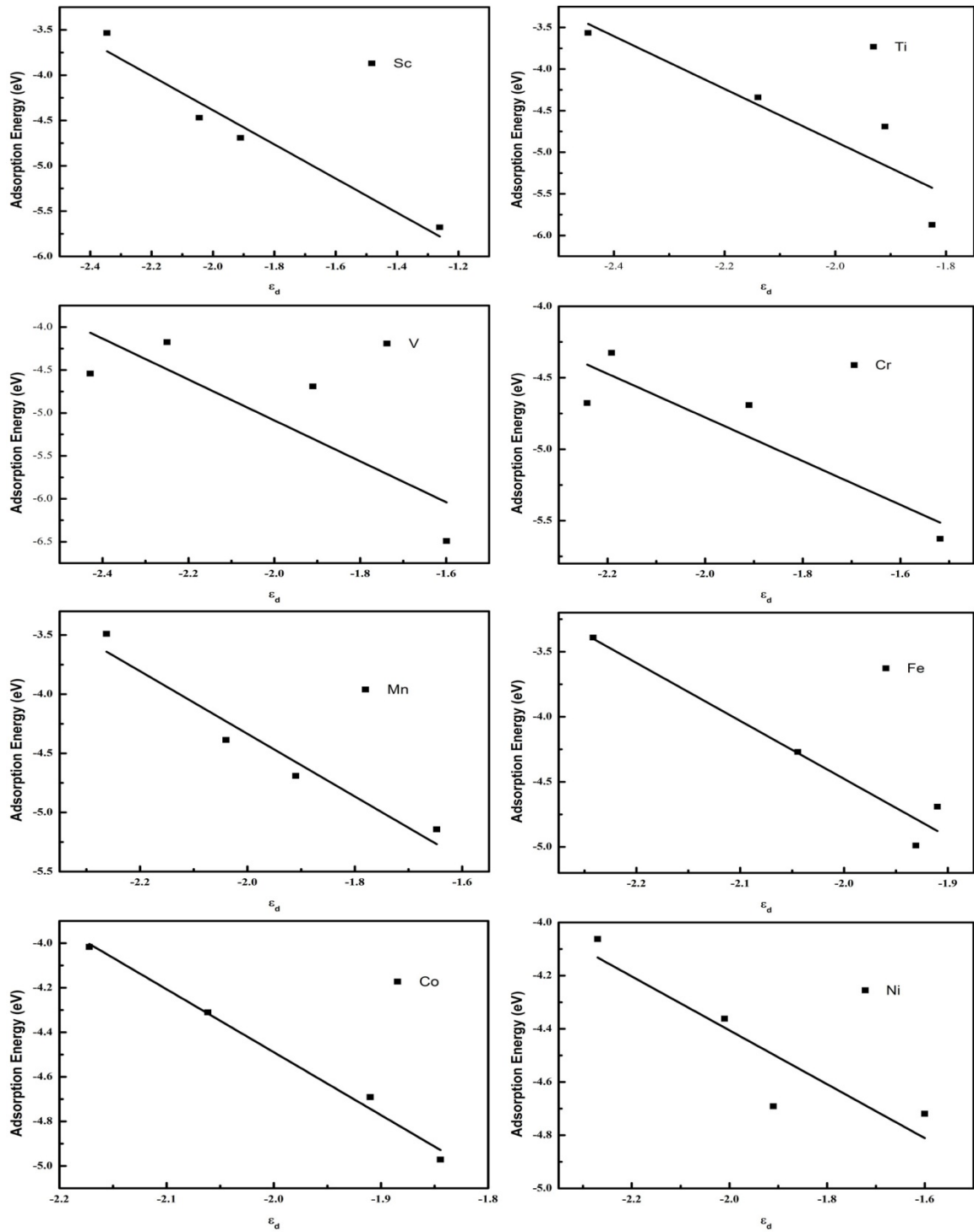


Fig. S2 The d-band center of top-layer atoms for the same Pt-M alloy system (M = Sc, Ti, V, Cr, Mn, Fe, Co, and Ni) with different alloy models.